

# Photometric observations and light curve solutions of the W UMa stars NSVS 2244206, NSVS 908513, CSS J004004.7+385531 and VSX J062624.4+570907

D. Kyurkchieva<sup>1</sup>, V. A. Popov<sup>2</sup>, D. Vasileva<sup>1</sup>, and N. Petrov<sup>3</sup>

<sup>1</sup> Department of Physics, Shumen University, 115, Universitetska Str., 1712 Shumen, Bulgaria;  
*d.kyurkchieva@shu-bg.net*

<sup>2</sup> IRIDA Observatory, 17A Prof. Asen Zlatarov str., Sofia, Bulgaria

<sup>3</sup> Institute of Astronomy and National Astronomical Observatory, Bulgarian Academy of Sciences, 72, Tsarigradsko Shose Blvd., 1784 Sofia, Bulgaria

Received ; accepted

**Abstract** Photometric observations in Sloan  $g'$  and  $i'$  bands of four W UMa stars, NSVS 2244206, NSVS 908513, CSS J004004.7+385531, VSX J062624.4+570907, are presented. The light curve solutions reveal that all targets have overcontact configurations with fillout factor within 0.15–0.26. Their components are of G-K spectral type and almost in thermal contacts. They are relatively close also in size and luminosity: the radius ratios  $r_2/r_1$  are within 0.75–0.90; the luminosity ratios  $l_2/l_1$  are within 0.53–0.63. The results of the light curve solution of CSS J004004.7+385531 imply weak limb-darkening effect of its primary component and possible presence of additional absorbing feature in the system.

**Key words:** methods: data analysis, stars: fundamental parameters, stars: binaries: eclipsing: individual (NSVS 2244206, NSVS 908513, CSS J004004.7+385531, VSX J062624.4+570907)

## 1 INTRODUCTION

W UMa-type binaries consist of two cool stars (F, G, K spectral type) in contact with each other, surrounded by a common convective envelope lying between the inner and outer critical Roche surfaces. In result their components possess almost identical surface brightness, i.e. temperature (Lucy 1968, Lucy 1976).

The periods of W UMa binaries are in the range 0.22–0.70 days. They present numerous family: around of 1/500–1/130 MS stars in the solar neighborhood (Rucinski 2002). There are many studies on them (Liu et al. 2011, Qian et al. 2013, Liao et al. 2014, etc.) but a complete theory of their origin, structure, evolution and future fate still lacks.

The most present theoretical models explain the formation of (short-period) contact systems by the systematic angular momentum loss (AML) in initially detached binaries with orbital periods of a couple of days, due to the magnetized stellar winds and tidal coupling (Vilhu 2014, Rahunen 1982, Stepień 1995). But according to Pribulla & Rucinski (2006) a third (distant) companion is necessary for formation of systems with a period under 1 day.

There are two models of the evolution during the contact phase itself. The thermal relaxation oscillation (TRO) model assumes that each component of the binary is out of thermal equilibrium and its size oscillates around the inner Roche lobe (Lucy 1976, Flannery 1976, Webbink 1977, Yakut & Eggleton 2005). The binary spends a part of its present life in contact (when both stars fill their Roche lobes and mass flows from the secondary to the primary) and the rest as a semi-detached binary (when only the primary fills its Roche lobe and mass flows from the primary to the secondary), slowly evolving towards an extreme mass ratio system. TRO model explains well the geometry of the W UMa-type stars: the primary component is an ordinary MS star and the secondary is also a MS star but swollen to its Roche lobe by energy transfer. The main problem of the TRO model is the mechanism of the energy transfer. The alternative model (Stepień 2004, Stepień 2006, Stepień 2009, Stepień 2011) assumes that mass transfer occurs with the mass ratio reversal, similarly as in Algol-type binaries, following the Roche lobe overflow (RLOF) by the massive component. The contact configuration is formed immediately after that or after some additional AML. Each component is in thermal equilibrium and the large size of the currently less massive component results from its advanced evolutionary stage (its core is hydrogen depleted).

The final products of the W UMa-type evolution are also debatable (Li et al. 2007, Eker et al. 2008). It is supposed that they may become: single blue stragglers (by merging of the W UMa components as a result of high rate of angular momentum loss); two brown dwarfs (Li et al. 2007) or two stars with very low mass (if mass-loss rate is very high).

The W-phenomenon is another unresolved problem and interesting peculiarity of the W UMa stars appearing by the lower apparent surface brightness of the more massive components of the W-type systems (Binnendijk 1970). They are recognized by the primary minima which are occultations (indicating that the small components are the hotter ones). It was suspected that this effect is due to a large coverage of the primary with cool, dark spots reducing significantly its apparent luminosity (Eaton et al. 1980, Stepień 1980, Hendry et al. 1992), but this explanation was not entirely convincing. Gazeas & Niarchos (2006) suggested that subtype A systems have higher total angular momentum (AM) and can evolve into subtype W which is the opposite of the earlier conclusion.

**Table 1** Previous information for our targets

Name	RA	Dec	Period	Epoch	V	Ampl	Type	Ref
			[d]	[d]	[mag]	[mag]		
NSVS 2244206	06 06 20.21	+65 07 21.0	0.280727	-	11.997	0.32	EB/EW	1
NSVS 908513	12 30 39.36	+83 23 07.8	0.399592	-	11.772	0.53	EB/EW	1
CSS J004004.7+385531	00 40 04.73	+38 55 31.9	0.251206	-	13.95	0.72	EW	2
VSX J004004.4+385513	00 40 04.40	+38 55 13.6	0.251206	2451359.756	13.42	0.34	EW	3
VSX J062624.4+570907	06 26 24.43	+57 09 07.4	0.280628	2455162.795	12.72	0.68	EW	3

References: 1 – [Gettel et al. \(2006\)](#); 2 – [Drake et al. \(2014\)](#); 3 – [Wozniak et al. \(2004\)](#);

**Table 2** Journal of the Rozhen photometric observations

Target	Date	Exposure ( $g'$ , $i'$ )	Number ( $g'$ , $i'$ )	Error ( $g'$ , $i'$ )
		[sec]		[mag]
NSVS 2244206	2015 Jan 8	60, 90	64, 64	0.004, 0.004
	2015 Jan 11	60, 90	78, 78	0.003, 0.004
	2015 Jan 12	60, 90	91, 84	0.004, 0.004
	2015 Jan 15	60, 90	147, 171	0.003, 0.003
NSVS 908513	2015 Mar 31	60, 90	55, 55	0.003, 0.004
	2015 Apr 11	60, 90	106, 144	0.002, 0.003
	2015 Apr 16	60, 90	138, 137	0.004, 0.005
CSS J004004.7+385531	2014 Nov 10	120, 120	110, 112	0.014, 0.014
	2014 Nov 20	120, 120	16, 16	0.011, 0.015
	2014 Nov 22	120, 120	44, 60	0.012, 0.014
	2014 Nov 26	120, 120	74, 66	0.008, 0.010
VSX J062624.4+570907	2014 Dec 24	150, 150	118, 117	0.003, 0.006

Besides their key role for understanding of the stellar evolution, the contact binaries are natural laboratories to study important astrophysical processes: interaction of stellar winds; magnetic activity; mass, energy and angular momentum transfer and loss; phenomenon "mass ratio reversal"; merging or fusion of the stars ([Martin et al. 2011](#)). The period-color-luminosity relation of the contact binary stars are an useful tool for distance determination ([Rucinski 1994](#), [Rucinski 1996](#); [Rucinski & Duerbeck 1997](#); [Klagyivik & Csizmadia 2004](#); [Eker et al. 2008](#)).

Hence, the study of the properties of the W UMa stars and their variety is important for the modern astrophysics. But the statistics of the most interesting W UMa stars, those with short periods, is still quite poor ([Terrell et al. 2012](#)) mainly due to their faintness (they are late stars).

In this paper we present photometric observations and light curve solutions of four short-period W UMa stars: NSVS 2244206, NSVS 908513, CSS J004004.7+385531  $\equiv$  2MASS J00400476+3855318  $\equiv$  GSC 02797-00705  $\equiv$  UCAC4-645-002474; VSX J062624.4+570907  $\equiv$  2MASS J06262444+5709075  $\equiv$  CSS J062624.5+570907  $\equiv$  GSC 03772-01134. Table 1 presents their coordinates and available (preliminary)

**Table 3** Coordinates and magnitudes of the standard and check stars

Label	Star ID	Other designations	RA	Dec	$g'$	$i'$
Target 1	NSVS 2244206	UCAC4 776-023507	06 06 20.21	+65 07 21.0	11.977	11.144
Chk	UCAC4 776-023451	GSC 04103-01161	06 05 04.84	+65 07 17.21	11.736	11.367
C1	UCAC4 777-021920	GSC 04103-00028	06 06 58.03	+65 18 15.55	13.905	12.452
C2	UCAC4 777-021910	GSC 04103-00908	06 06 39.95	+65 17 56.15	13.270	12.842
C3	UCAC4 777-021896	GSC 04103-00086	06 06 31.01	+65 15 33.41	12.338	11.895
C4	UCAC4 776-023478	GSC 04103-01089	06 05 43.92	+65 08 32.90	13.219	12.628
C5	UCAC4 776-023468	GSC 04103-01386	06 05 27.41	+65 03 00.31	12.335	11.802
C6	UCAC4 776-023541	GSC 04103-00274	06 06 57.18	+65 00 11.24	13.121	12.600
C7	UCAC4 775-024696	GSC 04103-00798	06 07 27.43	+64 59 18.52	12.602	11.433
C8	UCAC4 776-023570	GSC 04103-00108	06 07 39.47	+65 04 53.91	13.765	13.233
Target 2	NSVS 908513	UCAC4 867-006050	12 30 39.36	+83 23 07.8	11.772	11.105
Chk	UCAC4 867-006038	GSC 04633-01779	12 29 15.53	+83 20 58.94	13.285	12.466
C1	UCAC4 867-006016	GSC 04633-01264	12 25 15.86	+83 16 24.90	11.335	10.733
C2	UCAC4 867-006026	GSC 04633-01365	12 26 44.73	+83 15 13.74	11.088	10.747
C3	UCAC4 867-006048	GSC 04633-01496	12 30 02.21	+83 15 12.10	13.035	11.580
C4	UCAC4 867-006056	GSC 04633-01284	12 31 17.68	+83 22 11.16	13.786	12.918
C5	UCAC4 867-006057	GSC 04633-01516	12 31 39.72	+83 21 50.46	11.334	10.880
C6	UCAC4 868-005899	GSC 04633-01339	12 24 15.66	+83 27 36.10	12.305	11.610
C7	UCAC4 868-005922	GSC 04633-01435	12 28 54.40	+83 26 09.13	12.605	11.971
C8	UCAC4 868-005969	GSC 04633-01360	12 35 27.00	+83 26 58.19	12.049	10.779
C9	UCAC4 868-005942	GSC 04633-01599	12 31 56.99	+83 29 43.30	12.548	11.966
C10	UCAC4 868-005965	GSC 04633-01703	12 34 40.00	+83 32 27.62	12.985	12.260
C11	UCAC4 868-005971	GSC 04633-01424	12 35 37.57	+83 33 21.72	13.667	12.479
C12	UCAC4 868-005980	GSC 04633-01616	12 37 02.02	+83 32 47.47	11.259	10.850
Target 3	CSS J004004.7+385531	UCAC4 645-002474	00 40 04.73	+38 55 31.9	14.531	13.314
Chk	UCAC4 645-002460	GSC 02784-01714	00 39 51.35	+38 55 14.15	14.129	13.642
C1	UCAC4 645-002459	GSC 02784-00660	00 39 51.08	+38 52 47.94	13.984	13.560
C2	UCAC4 645-002487	GSC 02797-00707	00 40 16.35	+38 51 36.13	14.213	13.208
C3	UCAC4 645-002499	GSC 02797-00841	00 40 26.60	+38 55 17.97	14.117	13.528
C4	UCAC4 645-002488	GSC 02797-00759	00 40 16.49	+38 57 06.96	14.186	13.674
C5	UCAC4 645-002434	GSC 02784-00090	00 39 22.45	+38 55 07.13	13.935	13.808
C6	UCAC4 645-002509	GSC 02797-00433	00 40 41.68	+38 55 19.64	14.343	13.750
C7	UCAC4 644-002468	GSC 02784-01325	00 39 34.96	+38 42 54.15	13.725	13.214
C8	UCAC4 644-002496	GSC 02784-01757	00 39 59.82	+38 43 47.26	14.275	13.392
Target 4	VSX J062624.4+570907	UCAC4 736-046853	06 26 24.43	+57 09 07.4	13.413	12.469
Chk	UCAC4 737-044764	GSC 03773-00028	06 27 28.22	+57 14 51.82	13.912	12.355
C1	UCAC4 737-044774	GSC 03773-00266	06 27 41.41	+57 16 07.39	14.768	14.029
C2	UCAC4 737-044766	GSC 03773-00279	06 27 30.58	+57 16 07.12	14.517	13.872
C3	UCAC4 737-044778	GSC 03773-00030	06 27 48.83	+57 18 39.37	13.565	13.001
C4	UCAC4 736-046930	GSC 03773-00302	06 27 53.71	+57 11 14.10	13.344	12.349
C5	UCAC4 736-046874	GSC 03773-00004	06 26 46.16	+57 11 30.66	13.964	13.318
C6	UCAC4 736-046859	GSC 03772-01339	06 26 33.14	+57 04 49.70	13.514	12.656
C7	UCAC4 736-046863	GSC 03772-00447	06 26 36.42	+57 02 51.35	14.111	13.185
C8	UCAC4 736-046818	GSC 03772-01556	06 25 48.21	+57 08 54.91	13.787	12.977

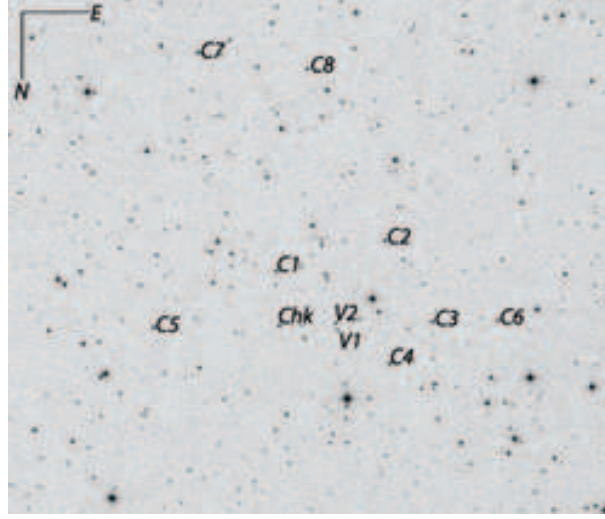


**Fig. 1** The field of CSS J004004.7+385531(V1) with the close star VSX J004004.4+385513 (V2) wrongly considered as a variable

## 2 OBSERVATIONS

Our CCD photometric observations of the targets in Sloan  $g'$ ,  $i'$  bands were carried out at Rozhen Observatory with the 30-cm Ritchey Chretien Astrograph (located into the *IRIDA South* dome) using CCD camera ATIK 4000M ( $2048 \times 2048$  pixels,  $7.4 \mu\text{m}/\text{pixel}$ , field of view  $35 \times 35$  arcmin). Information for our observations is presented in Table 2.

The photometric data were reduced by AIP4WIN2.0 (Berry & Burnell 2005). We performed aperture ensemble photometry with the software VPHOT using more than six standard stars in the observed field of each target. The coordinates and magnitudes of the standard and check stars (Table 3) were taken from the catalogue UCAC4 (Zacharias et al. 2013).

We established that there are two close objects, CSS J004004.7+385531 and VSX J004004.4+385513, with the same periods and types of variability in the VSX database (Table 1). Our observations revealed that the true variable is CSS J004004.7+385531 while VSX J004004.4+385513 is a stationary star (Fig. 1).

We determined the times of the individual minima (Table 4) by the method of Kwee & van Woerden (1956).

## 3 LIGHT CURVE SOLUTIONS

We carried out modeling of the photometric data by the code PHOEBE (Prsa & Zwitter 2005). It is based on the Wilson–Devinney (WD) code (Wilson & Devinney 1971, Wilson 1979). PHOEBE incorporates all the functionality of the WD code but also provides a graphical user interface alongside other improvements, including updated filters as Sloan ones used in our observations. We apply the traditional convention the MinI (phase 0.0) to be the deeper light minimum and the star that is eclipsed at MinI to be the primary (hotter) component.

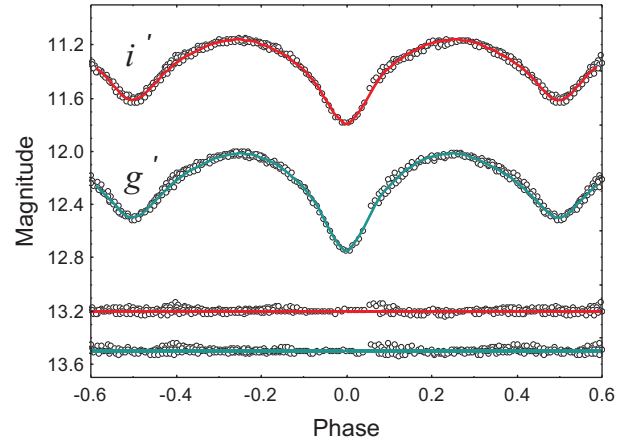


**Fig. 2** Top: the folded light curves of NSVS 2244206 and their fits; Bottom: the corresponding residuals (shifted vertically by different number to save space). Color version of this figure is available in the online journal.

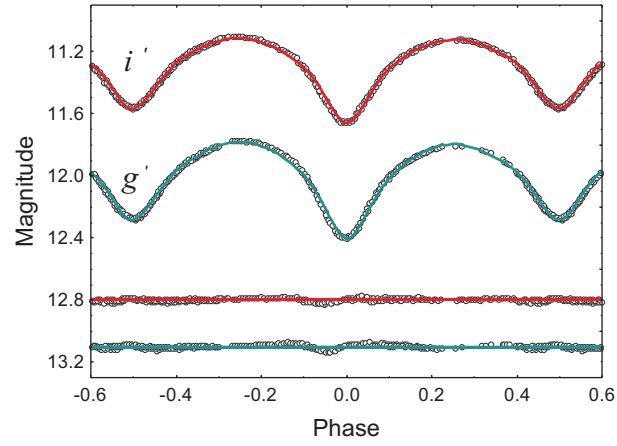


**Fig. 3** Same as Fig. 2 for NSVS 908513

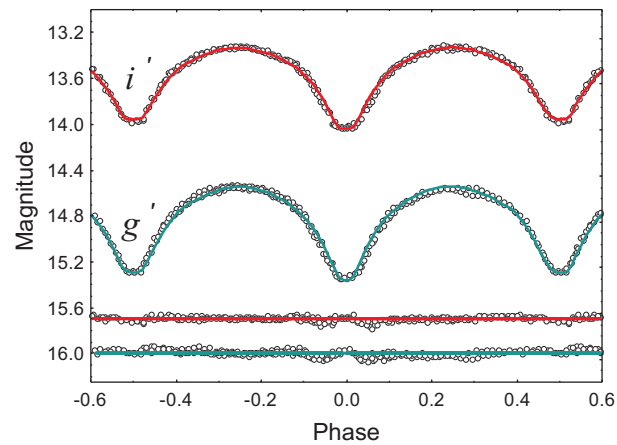


**Fig. 4** Same as Fig. 2 for CSS J004004.7+385531

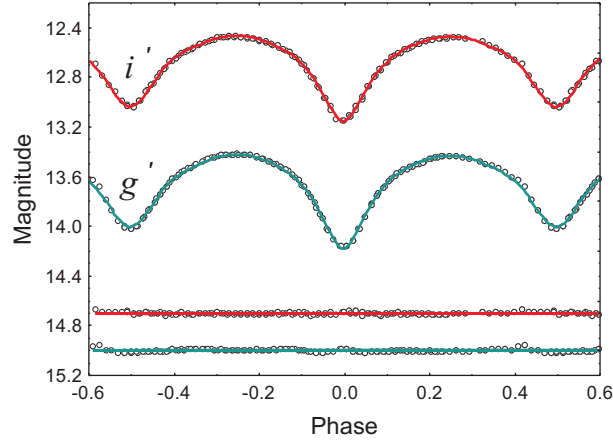


**Fig. 5** Same as Fig. 2 for VSX J062624.4+570907

**Table 4** Times of minima of our targets

Target	MinI	MinII
NSVS 2244206	-	2457033.51298
	-	2457034.35629
	-	2457038.28497
	2457038.42614	-
NSVS 908513	-	2457113.31730
	2457124.30454	2457124.50608
	2457129.50051	2457129.30045
CSS J004004.7+385531	2456972.34036	2456972.46714
	2456972.59113	2456982.26682
	2456984.39854	2456988.29364
	2456988.41840	-
VSX J062624.4+570907	2457016.33657	2457016.47792
	2457016.61853	-

We determined in advance the mean temperatures  $T_m$  of the binaries (Table 5) by their infrared color indices ( $J-K$ ) from the 2MASS catalog and the calibration color-temperature of [Tokunaga \(2000\)](#). In fact, the determination of stellar temperatures from the infrared flux is a method first developed by [Blackwell & Shallis \(1970\)](#).

Our procedure of the light curve solutions was carried out in several stages.

At the first stage we fixed  $T_1^0 = T_m$  and searched for fit varying the secondary temperature  $T_2$ , orbital inclination  $i$ , mass ratio  $q = m_2/m_1$  and potentials  $\Omega_{1,2}$  (and thus relative radii  $r_{1,2}$  and fillout factor  $f$ ). The fit quality was estimated by the value of  $\chi^2$ .

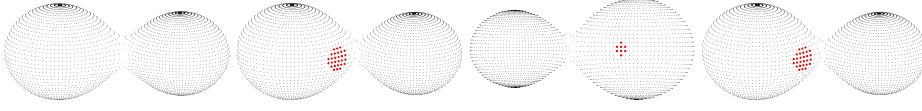


**Fig. 6** From the left to the right 3D configurations of: NSVS 2244206, NSVS 908513, CSS J004004.7+385531, VSX J062624.4+570907

Coefficients of gravity brightening and reflection effect appropriate for stars with convective envelopes were adopted. Initially we used linear limb-darkening law with limb-darkening coefficients corresponding to the stellar temperatures and Sloan photometric system (Claret & Bloemen 2011).

In order to reproduce the light curve distortions of the targets we added cool spots on the stellar surfaces and varied spot parameters: longitude  $\lambda$ , latitude  $\beta$ , angular size  $\alpha$  and temperature factor  $\kappa = T_{sp}/T_{st}$ .

As a result of the first stage of the light curve solution we obtained the values  $T_2^0$ ,  $i^0$ ,  $\Omega_{1,2}^0$ ,  $q$  as well as the spot parameters for each target.

After reaching the best fit we adjusted  $T_1$  and  $T_2$  around the value  $T_m$  by the formulae (Kjurkchieva et al. 2015)

$$T_1^c = T_m + \frac{c\Delta T}{c+1} \quad (1)$$

$$T_2^c = T_1^c - \Delta T \quad (2)$$

where  $c = l_2/l_1$  and  $\Delta T = T_1^0 - T_2^0$  are determined from the PHOEBE solution.

Finally, we varied slightly  $T_1$ ,  $T_2$ ,  $i$  and  $\Omega_{1,2}$  around their values  $T_1^c$ ,  $T_2^c$ ,  $i^0$  and  $\Omega_{1,2}^0$  and obtained the final PHOEBE solution.

The first part of Table 5 contains the parameters of our light curve solutions: mass ratio  $q$ ; orbital inclination  $i$ ; potentials  $\Omega_{1,2}$ ; fillout factor  $f$ ; stellar temperatures  $T_{1,2}$ ; relative radii  $r_{1,2}$ ; ratio of relative luminosities  $l_2/l_1$ . The errors of these parameters are the formal PHOEBE errors. Table 6 gives the obtained spot parameters. The synthetic curves corresponding to our light curve solutions are shown in Figs. 2-5.

Due to the lack of radial velocity measurements we had not a possibility to determine reliable values of the global parameters of the target components. We were able to obtain some estimations of these quantities by the following procedure.

The primary luminosity  $L_1$  was determined by the empirical relation luminosity-temperature for MS stars. The secondary luminosity  $L_2$  was calculated by the relation  $L_2 = cL_1$  where  $c = l_2/l_1$  is the luminosity ratio from our light curve solution.

We obtained the orbital separation  $a$  (in solar radii) from the equation

$$\log a = 0.5 \log L_i - \log r_i - 2 \log T_i + 2 \log T_\odot. \quad (3)$$

and then calculated the absolute stellar radii by  $R_i = ar_i$ .



**Table 5** Parameters of the best light curve solutions (top) and global parameters (bottom) of the targets

Star name	NSVS 2244206	NSVS 908513	CSS J004004.7+385531	VSX J062624.4+570907
$q$	$0.735 \pm 0.003$	$0.709 \pm 0.002$	$0.548 \pm 0.004$	$0.777 \pm 0.002$
$i, (^{\circ})$	$76.42 \pm 0.07$	$75.15 \pm 0.03$	$89.77 \pm 0.01$	$78.88 \pm 0.11$
$\Omega_1 = \Omega_2$	$3.1961 \pm 0.004$	$3.2 \pm 0.002$	$2.9 \pm 0.009$	$3.307 \pm 0.004$
$f$	$0.260 \pm 0.002$	$0.146 \pm 0.004$	$0.206 \pm 0.009$	$0.162 \pm 0.004$
$T_m, (K)$	5000	5810	4560	5230
$T_1, (K)$	$5157 \pm 36$	$5923 \pm 25$	$4560 \pm 37$	$5350 \pm 20$
$T_2, (K)$	$4702 \pm 32$	$5615 \pm 23$	$4560 \pm 38$	$5044 \pm 7$
$r_1$	$0.429 \pm 0.001$	$0.422 \pm 0.001$	$0.449 \pm 0.003$	$0.416 \pm 0.002$
$r_2$	$0.376 \pm 0.001$	$0.363 \pm 0.001$	$0.344 \pm 0.004$	$0.372 \pm 0.002$
$l_2/l_1$	0.5301	0.5946	0.5883	0.6314
$L_1^{bol}$	$0.519 \pm 0.023$	$1.031 \pm 0.023$	$0.254 \pm 0.04$	$0.604 \pm 0.073$
$L_2^{bol}$	$0.338 \pm 0.045$	$0.646 \pm 0.046$	$0.149 \pm 0.062$	$0.421 \pm 0.096$
$a, (R_{\odot})$	$2.214 \pm 0.06$	$2.312 \pm 0.066$	$1.798 \pm 0.055$	$2.23 \pm 0.067$
$R_1, (R_{\odot})$	$0.951 \pm 0.028$	$0.976 \pm 0.03$	$0.808 \pm 0.03$	$0.927 \pm 0.032$
$R_2, (R_{\odot})$	$0.833 \pm 0.032$	$0.839 \pm 0.033$	$0.619 \pm 0.026$	$0.829 \pm 0.027$
$M_1, (M_{\odot})$	$1.064 \pm 0.084$	$0.607 \pm 0.051$	$0.798 \pm 0.07$	$1.061 \pm 0.094$
$M_2, (M_{\odot})$	$0.782 \pm 0.067$	$0.430 \pm 0.038$	$0.437 \pm 0.043$	$0.825 \pm 0.077$

The total target mass  $M$  (in solar units) was calculated from the third Kepler law

$$M = \frac{0.0134a^3}{P^2} \quad (4)$$

where  $P$  is in days while  $a$  is in solar radii. Then the individual masses  $M_i$  were determined by the formulae  $M_1 = M/(1+q)$  and  $M_2 = M - M_1$ .

The global parameters of the target components obtained by the foregoing procedure are given in the second part of Table 5. Their errors are calculated from the corresponding formulae by the errors of the quantities of the light curve solutions or observations.

#### 4 ANALYSIS OF THE RESULTS

The analysis of the light curve solutions of our short-period W UMa stars led to several important results.

(1) CSS J004004.7+385531 reveals total eclipses while the remained three targets undergo partial eclipses.

(2) The temperatures of the stellar components of the targets correspond to G-K spectral type (Table 5). The temperature differences of their components do not exceed 450 K while the components of CSS J004004.7+385531 are in precise thermal contact.

(3) The targets have overcontact configurations which fillout factors  $f$  are in the range 0.15–0.26 (Table 5). It should be pointed out that the preliminary classification of NSVS 2244206 and NSVS 908513 was EB/EW (Table 1) but our observations and light curve solutions led to the conclusion that their configurations are overcontact (Fig. 6).

(4) The target components are relatively close in size and luminosity: the size ratios  $r_2/r_1$  are within 0.75–0.90; the luminosity ratios  $l_2/l_1$  are within 0.53–0.63.

(5) We observed slightly different levels of the two quadratures (O’Connell effect) of three our targets. They were reproduced by small cool spots (Table 6) on their primaries. We obtained solutions with the same fit quality for combinations of slightly different spot sizes (within  $1^\circ$ ) and latitudes ( $\pm 25^\circ$  around the stellar equator). Table 6 presents the parameters of the equatorial spots whose angular sizes have minimum values.

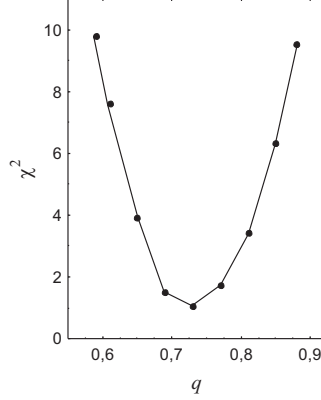
(6) The residuals of CSS J004004.7+385531 are bigger than those of the other three targets that is expected taking into account that this totally-eclipsed binary is the faintest member of our sample (Table 1). But the residuals are biggest at its primary eclipse because the synthetic eclipse is narrower than the observed one (Fig. 4). The reason for this discrepancy is that the observed primary eclipse of CSS J004004.7+385531 turns out slightly wider than the secondary one. This may due to some additional structure in the system which presence cannot be taken into account from the software for light curve synthesis: equatorial bulge around the less massive component (accretor) formed as a result of the transferred mass; disk-like feature; clouds at some Lagrangian points (result of previous nonconservative mass transfer, [Stepien & Kiraga 2013](#)).

(7) We managed to reproduce the almost flat bottom of the primary eclipse of CSS J004004.7+385531, especially in  $i'$  band, only by very small limb-darkening coefficient of 0.18, a value considerably smaller than that corresponding to its temperature. This formally means faint limb-darkening effect, i.e. almost homogeneous stellar disk of the primary component. There are two possible reasons for this effect. The first one is that the theory and corresponding codes for light curve synthesis cannot take into account precisely the limb-darkening effect for overcontact binaries with strongly distorted components whose photospheres are deeply inside the envelopes. The second reason for the flat bottom of the primary eclipse might be light contribution of optically thick region around L1 that is covered by the secondary component at the primary eclipse. Such an argument refers just for CSS J004004.7+385531 that undergoes almost central eclipse.

(8) Quite often photometric solutions of W UMa light curves appear to be ambiguous since both A and W configurations can fit well the observations ([van Hamme 1982a](#); [Lapasset & Claria 1986](#)). The mass ratio of the W UMa binaries is important parameter for their W/A subclassification. But the rapid rotation of their components does not allow to obtain precise spectral mass ratio from measurement of their highly broadened and blended spectral lines ([Bilir et al. 2005](#); [Dall & Schmidtobreick 2005](#)). As a result the W/A subclassification of the W UMa binaries is made mainly on the widely-accepted empirical relation “spectral type – mass” ([van Hamme 1982a](#); [Lapasset & Claria 1986](#)): the G-K binaries are of W subtype while A and earlier F binaries are of A subtype.

**Table 6** Parameters of the cool spots on the targets

Target	$\beta$	$\lambda$	$\alpha$	$\kappa$
NSVS 908513	90	330	13	0.90
CSS J004004.7+385531	90	70	7	0.90
VSX J062624.4+570907	90	270	10	0.90

**Fig. 7** Sensibility of our light curve solution of NSVS 2244206 (measured by  $\chi^2$ ) to the mass ratio (the rest parameters last fixed at their final values)

Particularly, our targets are faints objects and we have obtained only their photometric mass ratios  $q$  by varying this parameter within the range 0.1-2.5. Thus, we obtained a pair solutions for each target with close quality: (a) A-subtype solution with parameters  $q^A < 1$ ,  $r_1^A, r_2^A < r_1^A$ ; (b) W-subtype solution with parameters  $q^W \approx 1/q^A$ ,  $r_1^W \approx r_2^A$ ,  $r_2^W \approx r_1^A$ . To choose one of them we introduced the relative difference  $\Delta Q$  (in percentage) of the solution quality  $Q(W)$  corresponding to the W-subtype configuration and the solution quality  $Q(A)$  corresponding to the A-subtype configuration

$$\Delta Q = \frac{Q(W) - Q(A)}{Q(A)}. \quad (5)$$

For all our targets we established  $\Delta Q \geq 3\%$ , i.e. the A solutions are better than the W solutions. This allowed us to assume that A subtype is more probable subclassification of our targets than the W subtype. Additional considerations for this choice were: (i) the W solutions did not reproduce so good the observed eclipse depths; (ii) the big fillout factors of our targets are inherent to A subtype binaries (van Hamme 1982a, van Hamme 1982b); (iii) the A solutions are quite sensible to the mass ratio (Fig. 7).

Hence, our targets could be assigned to the exceptions from the statistical relation "spectral type – mass". The possible reason for this discrepancy may be that this relation is derived for W UMa binaries with periods  $> 0.3$  d (van Hamme 1982a, van Hamme 1982b).

## 5 CONCLUSION

We obtained light curve solutions of four short-period W UMa binaries which main results are as follows.

(1) The temperatures of the stellar components of the targets correspond to G-K spectral type and they are almost in thermal contacts.

(2) All targets are overcontact configurations with fillout factor within 0.15–0.26.

(3) The target components are relatively close in size and luminosity: the size ratios  $r_2/r_1$  are within 0.75–0.90; the luminosity ratios  $l_2/l_1$  are within 0.53–0.63.

(4) The results of the light curve solution of CSS J004004.7+385531 imply weak limb-darkening effect of its primary component and possible presence of additional absorbing feature in the system.

This study adds new four systems with estimated parameters to the family of short-period binaries. They could help to improve the statistical relations between the stellar parameters of the low-massive stars and to better understanding the evolution of close binaries.

**Acknowledgements** The research was supported partly by funds of project RD 08-244 of Scientific Foundation of Shumen University. It used the SIMBAD database and NASA Astrophysics Data System Abstract Service. This research was made possible through the use of the AAVSO Photometric All-Sky Survey (APASS), funded by the Robert Martin Ayers Sciences Fund. The authors are grateful to the anonymous referee for the valuable notes and recommendations.

## References

- Berry, R., & Burnell, J. 2005, The handbook of astronomical image processing, 2nd ed., by R. Berry and J. Burnell. xxviii, 684 p., 1 CD-ROM (incl. Astronomical Image Processing Software AIP4WIN, v.2.0). Richmond, VA: Willmann-Bell, 2005 [5](#)
- Bilir, S., Karatas, Y., Demircan, O., & Eker, Z. 2005, MNRAS, 357, 497 [10](#)
- Binnendijk, L. 1970, Vistas in Astronomy, 12, 217 [2](#)
- Blackwell, D., & Shallis, M. 1970, Vistas in Astronomy, 12, 217 [7](#)
- Claret, A., & Bloemen, S. 2011, Astronomy & Astrophysics, 529, 75 [8](#)
- Dall, T. H., & Schmidtbreick, L. 2005, A & A, 429, 625 [10](#)
- Drake, A. J., Djorgovski, S. G., Garcia-Alvarez, D., et al. 2014, ApJ, 790, 157 [3](#)
- Eaton, J., Wu, C., & Rucinski, S. 1980, ApJ, 239, 919 [2](#)
- Eker, Z., Demircan, O., & Bilir, S. 2008, MNRAS, 386, 596 [2](#), [3](#)
- Flannery, B. P. 1976, ApJ, 205, 217 [2](#)
- Gazeas, K., & Niarchos, P. 2006, Monthly Notices of the Royal Astronomical Society: Letters, 370, L29 [2](#)
- Gettel, S. J., Geske, M. T., & McKay, T. A. 2006, AJ, 131, 621 [3](#)
- Hendry, P., Mochnacki, S., & Collier Cameron, A. 1992, ApJ, 399, 246 [2](#)
- Kjurkchieva, D., Popov, V., Petrov, N., & Ivanov, E. 2015, Contributions of the Astronomical Observatory Skalnat Pleso, 45, 28 [8](#)

- Kwee, K. K., & van Woerden, H. 1956, *Bulletin of the Astronomical Institutes of the Netherlands*, 12, 327 5
- Lapasset, E., & Claria, J. J. 1986, *Astronomy and Astrophysics*, 161, 264 10
- Li, L., Zhang, F., Han, Z., & Jiang, D. 2007, *ApJ*, 662, 596 2
- Liao, W. P., Qian, S. B., Zhao, E. G., & Jiang, L. Q. 2014, *New Astronomy*, 31, 65 2
- Liu, L., Qian, S. B., Zhu, L. Y., et al. 2011, *PASP*, 415, 3006 2
- Lucy, L. B. 1968, *ApJ*, 151, 1123 1
- Lucy, L. B. 1976, *ApJ*, 205, 208 1, 2
- Martin, E. L., Spruit, H. C., & Tata, R. 2011, *A & A*, 535, A50 3
- Pribulla, T., & Rucinski, S. 2006, *The Astronomical Journal*, 131, 2986 2
- Prsa, A., & Zwitter, T. 2005, *ApJ*, 628, 426 5
- Qian, S. B., Li, K., & Liao, W. P. 2013, *AJ*, 145, 6 2
- Rahunen, T. 1982, *Astronomy and Astrophysics*, 109, 66 2
- Rucinski, S., & Duerbeck, H. 1997, *Publications of the Astronomical Society of the Pacific*, 109, 1340 3
- Rucinski, S. M. 1994, *Astronomical Society of the Pacific*, 106, 462 3
- Rucinski, S. M. 1996, *ASPC*, 90, 508 3
- Rucinski, S. M. 2002, *PASP*, 114, 1124 2
- Stepien, K. 1980, *Acta Astronomica*, 30, 315 2
- Stepien, K. 1995, *Monthly Notices of the Royal Astronomical Society*, 274, 1019 2
- Stepien, K. 2004, *IAUS*, 219, 967 2
- Stepien, K. 2006, *AcA*, 56, 199 2
- Stepien, K. 2009, *MNRAS*, 397, 857 2
- Stepien, K. 2011, *AcA*, 61, 139 2
- Stepien, K., & Kiraga, M. 2013, *AcA*, 63, 239 10
- Terrell, D., Gross, J., & Cooney, W. R. 2012, *AJ*, 143, 99 3
- Tokunaga, A. T. 2000, *Allen's astrophysical quantities*, 4th ed. Edited by Arthur N. Cox. ISBN: 0-387-98746-0. Publisher: New York: AIP Press; Springer, 143 7
- van Hamme, W. 1982a, *Astronomy and Astrophysics*, 116, 27 10, 11
- van Hamme, W. 1982b, *Astronomy and Astrophysics*, 105, 389 11
- Vilhu, O. 2014, *Astrophysics and Space Science*, 78, 401 2
- Webbink, R. F. 1977, *ApJ*, 215, 851 2
- Wilson, R. 1979, *Astrophysical Journal*, 234, 1054 5
- Wilson, R., & Devinney, E. 1971, *Astrophysical Journal*, 166, 605 5
- Wozniak, P. R., Vestrand, W. T., Akerlof, C. W., et al. 2004, *AJ*, 127, 2436 3
- Yakut, K., & Eggleton, P. 2005, *ApJ*, 629, 1055 2
- Zacharias, N., Finch, C., Girard, T., et al. 2013, *The Astronomical Journal*, 145, 14 5

